كلية الهندسة بشبرا
FACULTY OF ENGINEERING AT SHOUBRA
ERJ
ISSN:1687-1340

ENGINEERING RESEARCH JOURNAL (ERJ)
Volume (52) , Issue (2)
April 2023, pp:81-100
https://erjsh.journals.ekb.eg

Numerical Investigation of RC Beams Reinforced With Geo-grid And Steel Fiber in The Flexural Zone

Mona K. N. Ghali[a], Ahmed Mohamed Salah EL-din[a], Sherif Ahmed ELbeshlawy[b], and Mariam Mostafa*[b].

[a] Department of Civil Engineering, Faculty of Engineering at Shoubra Benha University
b Department of Construction and Building Engineering, The Higher Institute Of Engineering 6th October, Giza, Egypt
* Corresponding Author
E-mail : mariammostafa20153@gmail.com,mnghali@gmail.com,engahmed77@yahoo.com,beshlawys@yahoo.com.

Abstract: Geo-grid is a material manufactured from polymers and classified as a geo-synthetic material. Nowadays, using geo-grid in reinforced concrete members sets a new beginning in employing geosynthetic materials in structural engineering. This research work describes a comparative study of RC beams reinforced with uniaxial geogrid and steel fibers in the presence of flexural reinforcement. Eleven experimentally tested reinforced concrete beams were chosen to verify this work. ANSYS program was used in the analysis of the beams. Concrete is modeled as solid element (SOLID65), whereas geo-grid and steel fibers were modeled as volumetric ratios. A parametric study was carried out using eighty-five reinforced concrete beams. The eighty-five beam specimens may be classified into fifteen groups. They were modeled using ANSYS Vr (15.0) nonlinear finite element program. The main studied parameters were the compressive strength, different volumes of steel fibers, different values of geo-grid volumetric ratio (3, 4.5, 6, 7.5, and 9%), and different Bottom Reinforcement Ratios. Addition of uniaxial geo-grids as a reinforcing technique proved to be an effective tool to improve the flexural behavior of beams and improve the cracking patterns. Increasing the geogrid volumetric ratio in reinforced concrete beams plays a major role in ameliorating their flexural behavior.

Keywords: RC, Beams, Geo-grid, and ANSYS.

1. INTRODUCTION

Geo-grids are employed as reinforcing and stabilization materials in different civil engineering and infrastructure works. Geo-grids were first utilized as reinforcement to improve the concrete overlay performance. The presence of micro cracks in the aggregate interface of mortar is responsible for the weakness inherent in plain concrete. Inclusion of fibers in the concrete mixture can overcome this weakness. Steel fiber (SF) is the most popular fiber used as concrete reinforcement. The function of steel fibers is summarized as follows: when the cracks start to appear in the concrete; the randomly oriented fibers start operating, holding cracks formation and diffusion. Thus, it improves the ductility and strength of the concrete and increases its flexural toughness, energy absorption capacity, and reduces cracking. The study investigates the possibility of improving the behavior of the beams by adding uniaxial geogrid and randomly spread steel fibers in the concrete mixture.

2.Research Objective

Limited research work has been carried out to investigate the flexural behavior of reinforced concrete beams additionally reinforced with Geo-grids. This theoretical study aims to investigate the behavior of RC beams reinforced with steel reinforcement, and additionally reinforced with uniaxial geogrid and steel fibers. A finite element analysis (FEM) has been carried out using the ANSYS APDL program (v15). Verification of the theoretical work has been carried out using reported experimental results. In addition, a parametric study has been done to investigate the importance of different factors on the flexural behavior of this type of beams.

3.Literature Review

Saranydevi M et al. (2016): This paper aimed to use geotextile fabric and geo-grids in concrete beams in the flexural zone. A total of 18 beams with dimensions (150 x 100 x 1200) mm samples were divided into two parts. Nine

were tested after seven days of curing, and the rest of the specimens were tested after 28 days curing. Six reinforced concrete beams were strengthened with one layer of geo-grid in the flexural zone and six reinforced concrete beams were wrapped externally with geotextile fabric. Six beams were used as control specimens to investigate the strengthened behavior using the ANSYS program V14.5. The results indicated that the beams strengthened with geogrid or geotextile fabric around and inside the beams were found to be of extra effective perfection in improving the ultimate load-carrying capacity of the beams. The flexural strength of the concrete beams strengthened with geogrid materials gives better results than the conventional beams.

R. Siva and Pankaj Agarwal (2019): This research work explained the increased shear carrying capacity with a more suitable elastic response to reflect geo-grid benefits in RC structural elements. An experimental research work was carried out under static and cyclic loading to investigate the shear resistance capacity of RC beams and joints with geo-grid containment and steel fibers. The composite benefits of using minimum percentage (%) of steel fiber with geo-grid in the resistance of beam and base column joint specimens with improved stirrup spacing are investigated in detail. Besides, the improved energy dissipation and good composite action damage tolerance offered by geo-grid and steel fiber show the synergetic result in the resistance to shear forces in RC beams and beam column joints.

Özkal FM (2021): This research work studied the applicability of geogrid in reinforced concrete structural members. An experimental study was carried out to study hybrid-reinforced deep beams with web openings. This type of RC member has been selected to study the shear behavior of geo-grid material in RC structural members. Geogrid was used as the web reinforcement to produce conjugates of the conventionally designed beams in addition to the traditional beams. Observation of the tested beams revealed that geogrid was found to be effective when it is used as a reinforcement material. This study is important for the applicability and benefits of geogrid reinforcement in RC structural systems, mainly in which shear behavior is an initial problem.

4. Experimental study

(Mona K.N Ghali et al. 2022) conducted an experimental research work on thirteen RC beams having dimensions of 150 mm width, 300 mm depth, and 2100 mm length. The beams were simply supported with a 1900 mm clear span, as shown in Fig. (1). All details of reinforcement beams are shown in Table (1).

4.1 Specimen details

The specimens were divided into control beams (B1 and B2) in addition to three groups as follows:

- **Group (A)** consisted of beams (B3, B4, B5) reinforced with two bars bottom reinforcement of diameter 10 mm, having steel fiber VF (1)% and different numbers of geogrid layers (one, two, and three) layers. These layers were inserted in the tension zone with a spacing of 8 mm. The top reinforcement consisted of two bars with a diameter of 10 mm for all the beams. The stirrups consisted of two vertical branches of 8 mm diameter spaced at 100 mm to prevent shear failure.
- **Group (B)** consisted of beams (B6, B7, B8) reinforced with two bars of top reinforcement of diameter 10 mm, and reinforced with three bars bottom reinforcement, 3 phi 12 mm having a steel fiber VF (1) % and different numbers of geo-grid layers are laid in the tension zone with a spacing of 8mm (none, one, and two) layers. These layers were inserted in the tension zone with a spacing of 8 mm. The stirrups in all the beams consisted of two vertical branches of 8 mm diameter steel bars spaced at 100 mm.
- **Group (C)** consisted of (B9, B10, and B11) reinforced with two bars of bottom reinforcement of diameter 10 mm, having steel fiber VF (0.5) % and different numbers of geo-grids layers (one, two, and three) layers were inserted. These layers were inserted in the tension zone with a spacing of 8 mm. The top reinforcement were two bars with a diameter of 10 mm for all the beams. The stirrups consisted of two vertical branches of 8 mm diameter, spaced at 100 mm.

5. ANSYS Finite Element Model

The finite element program (ANSYS V15) was used to model the reinforced concrete beams.

5.1 Element types

In the present work, (SOLID65) was used to model concrete material, (SOLID185) was used to model the loading and supporting steel plates and (LINK 180) element was used to model steel reinforcement bars.

5.2 Real Constant

Solid 185 elements have no real constant. LINK 180 has the main real constant, which is the cross-sectional area. The uniaxial geogrid and steel fiber is modelled as a volumetric ratio in the concrete element, including the material number, the volume ratio, and the orientation angles for steel fiber and geogrid.

6. Analysis

Numerical results obtained for the beams were compared with the experimental results. FEM provides different types of advanced analysis, such as static, dynamic, linear and non-linear, supported by the ANSYS program.

The dimensions for the concrete volume in ANSYS are indicated in Table (2), while the volumes created in ANSYS APDL are shown in Fig. (2).

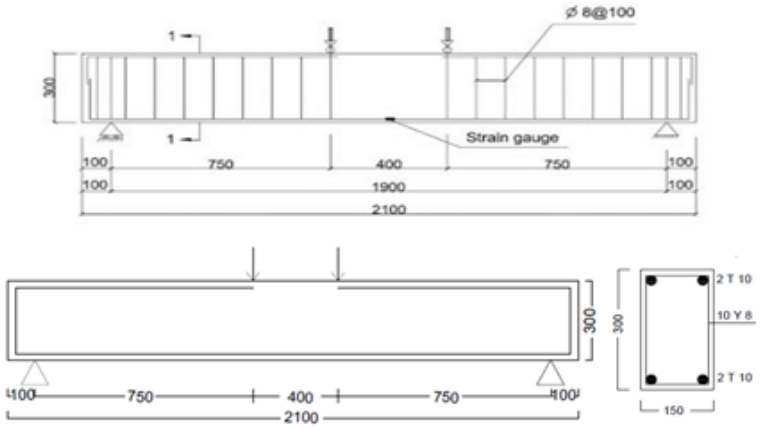

Fig 1. Reinforcement Details For All Tested Beams

Table 1. Tested specimens classification

Group	Specimen	No of layer (geogrid)	Fiber content Vf (%)	Bottom RFT	Top RFT	Stirrups
Control	B1	----	0%	2 ø 10	2 ø 10	10 ø 8
	B2		1%	2 ø 10	2 ø 10	10 ø 8
A	B3	1	1%	2 ø 10	2 ø 10	10 ø 8
	B4	2	1%	2 ø 10	2 ø 10	10 ø 8
	B5	3	1%	2 ø 10	2 ø 10	10 ø 8
B	B6	----	1%	3 ø 12	2 ø 10	10 ø 8
	B7	1	1%	3 ø 12	2 ø 10	10 ø 8
	B8	2	1%	3 ø 12	2 ø 10	10 ø 8
C	B9	1	0.5%	2 ø 10	2 ø 10	10 ø 8
	B10	2	0.5%	2 ø 10	2 ø 10	10 ø 8
	B11	3	0.5%	2 ø 10	2 ø 10	10 ø 8

Table 2. Dimensions for Concrete, Steel Plates, and Steel Supports Volumes in ANSYS APDL

IN ANSYS	Concrete (mm)		Steel plates (mm)				Steel supports (mm)			
			1		2		1		2	
X1, X2	0	2100	750	850	1250	1350	50	150	1950	2050
Y1, Y2	0	300	300	325	300	325	0	-25	0	-25
Z1, Z2	-75	75	-75	75	-75	75	-75	75	-75	75

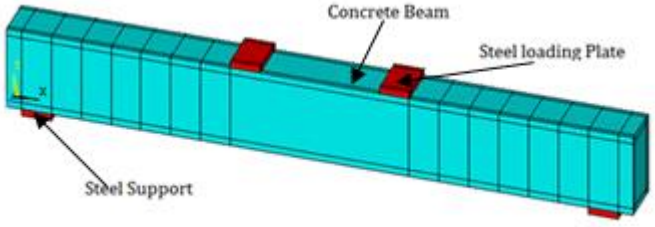

Fig 2. Volumes Created In ANSYS APDL V 15

.

Table 3. Comparison between the experimental (Exp.) and finite element (FEA) results.

`Group	SPECIMEN	LOAD Pu (KN)			DEFLECTION (at the same load level) Δ (mm)			FIRST CRACK LOAD Pcr (KN)		
		FEA	Exp.	FEA/ EXP.	FEA	Exp.	FEA/ EXP.	FEA	Exp.	FEA/ EXP.
Control	B1	75.6	77	0.98	3.8	5.42	0.70	23.4	30	0.78
	B2	90	82	1.09	5.7	7.3	0.78	23.4	42	0.56
A	B3	86.4	88	0.98	6.7	7.8	0.86	23.4	45	0.52
	B4	93.6	95	0.99	6.06	7.23	0.84	23.4	47	0.50
	B5	99	101	0.98	4.76	5.9	0.81	22	51	0.43
B	B6	133.	142	0.94	24.22	22.03	1.09	20	65	0.36
	B7	144	146	0.99	4.9	7.5	0.65	41.4	69	0.60
	B8	151.	153	0.99	4.9	6.7	0.73	43.2	72	0.60
C	B9	79.2	84	0.94	4.25	5.4	0.79	23.4	35	0.67
	B10	93.6	89	1.05	4.69	6.09	0.77	23.4	39	0.60
	B11	97.2	94	1.03	4.23	5.71	0.74	30.6	44	0.70

6.1 Load-deflection behavior

Fig.'s (3 to 13) illustrate the load-deflection curves for all the beams obtained from the experimental results and finite element models. As shown in table (3), the numerical model underestimated the ultimate strength of B1 by 1.8% compared with the experimental testing, while it overestimated the ultimate strength of B2 by 8.9% compared with experimental results. Comparison between experimental and FEA for the rest of the beams are summarized as follows:

- **Group (A)** of beams (B3, B4 and B5): By increasing the number of geogrid layers in group A, the deflection of B4 and B5 was decreased compared to B3.
  The analytical model underestimated the ultimate strength of the beams by 1.8%, 1.5% and 2 %, respectively, compared with the experimental tests.
  In this group, the ratio between the FEM to the experimental results of the deflection, at same load level, varies from 0.81 to 0.86. The ratio between the FEM compared to the experimental results of the ultimate load varies from 0.98 to 0.99.
- **Group (B)** of beams (B6, B7 and B8): By increasing the number of geogrid layers in group B the deflection of B7 and B8 was decreased compared to B6. The analytical model underestimated the ultimate strength by 6.2%, 1.4% and 1.2 %, respectively, compared with the experimental testing.
  The ratio between the FEM to the experimental results of the deflection, (at same load level) varies from 0.65 to 1.09. The ratio between the FEM compared to the experimental results of the ultimate load varies from 0.94 to 0.99.
- **Group (C):** of beams (B9, B10 and B11). By increasing the number of geogrid layers in group C the deflection of B10 and B11 was decreased compared to B9. The numerical model underestimated the ultimate strength of B9 by 5.7% and overestimated it in B10 and B11 by 5% and 3.3% compared with the EXP. results the ratio between the FEM to the experimental results of the deflection, at same load level, varies from 0.74 to 0.79. The ratio between the FEM compared to the experimental results of the ultimate load varies from 0.94 to 1.05. The load-deflection curve from modelling the beams by ANSYS reveals that the numerical model efficiently predicts the ultimate strength and corresponding displacement compared with experimental results. The curve has an approximate uniform linear ascending line until the ultimate load. The numerical calculation ended at the point of the ultimate load because the used stress-strain curve doesn't include concrete post behavior.

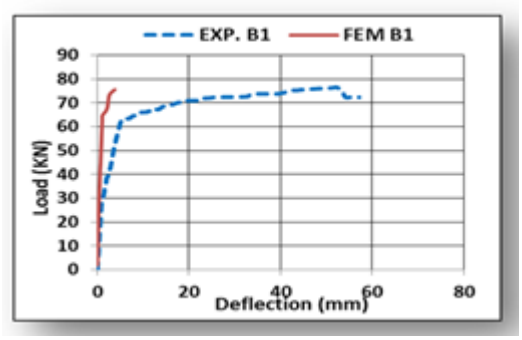

Fig 3. Load-deflection curve from FEM and EXP. work for B1 (control)

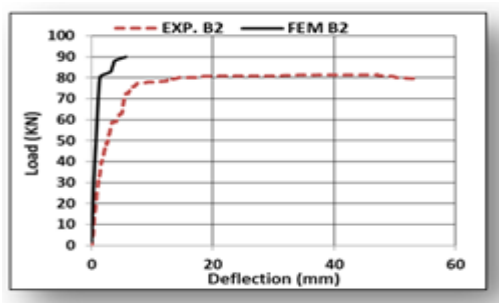

Fig 4. Load-deflection curve from FEM and EXP. work for B2

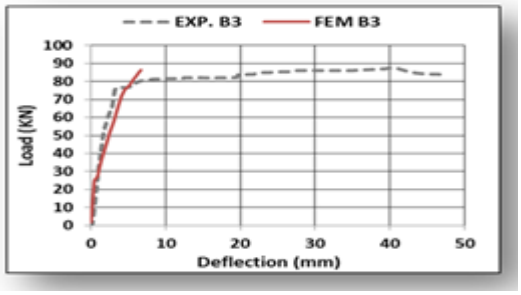

Fig 5. Load-deflection curve from FEM and EXP. work for B3

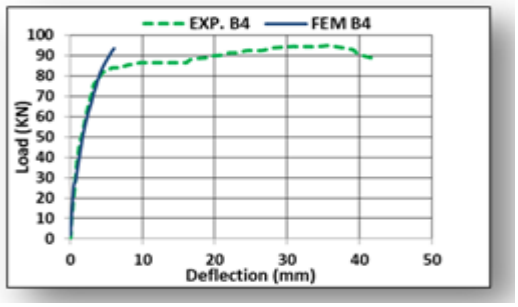

Fig 6. Load-deflection curve from FEM and EXP. work for B**4**

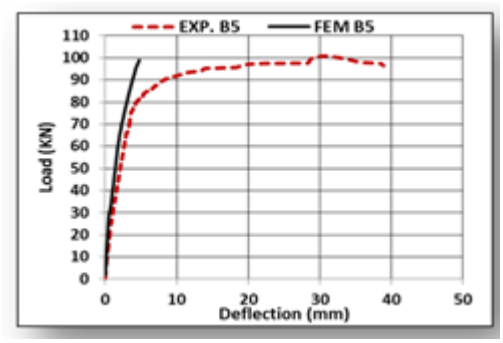

Fig 7. Load-deflection curve from FEM and EXP. work for B5

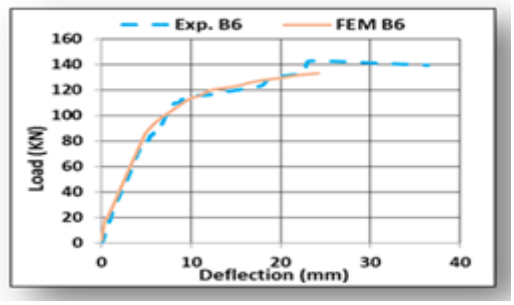

Fig 8. Load-deflection curve from FEM and EXP. work for B6

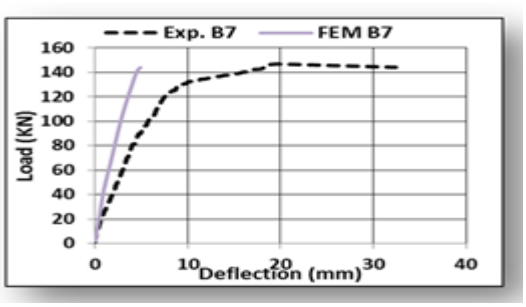

Fig 9. Load-deflection curve from FEM and EXP. work for B7

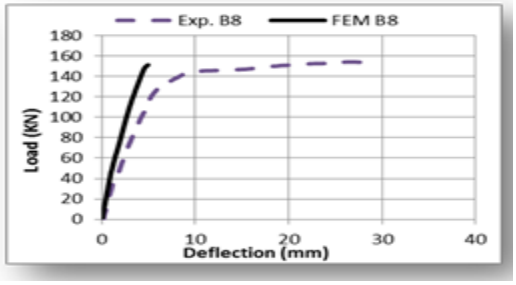

Fig 10. Load-deflection curve from FEM and EXP. work for B8

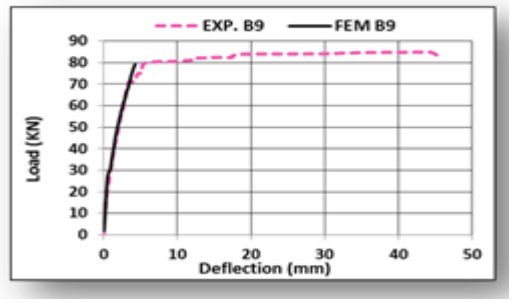

Fig 11. Load-deflection curve from FEM and EXP. work for B9

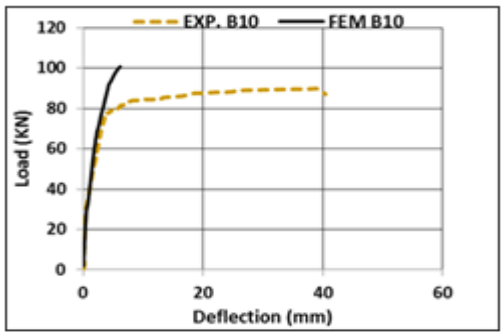

Fig 12. Load-deflection curve from FEM and EXP. work for B10

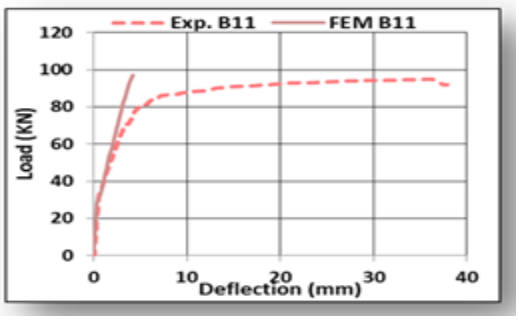

Fig 13. Load-deflection curve from FEM and EXP. work for B11

6.2 Failure modes:

6.2.1 Effect of the addition of geogrid on the failure loads:

A comparison between the failure loads in the FEM and EXP is shown in Fig.14.

- The failure load of **group (A)** in FEM decreased by 4% for beam B3 and increased by 4% and 10% for beams B4 and B5, respectively, compared to B2; whereas the failure load of **group (A)** in the experimental results increased by (7.3, 15.9 and 23.2%) for these beams.
- The failure load of **Group (C)** for beams B10 and B11 in FEM results increased by (4% and 8%), respectively and decreased by 11.6% for beam B9; compared to the control beam B2; whereas the experimental results increased by (2.5, 8.5 and 14.6%) for these beams respectively.
- **Group (B)**: The failure loads for this group increased by 48%, 60% and 68% for beams B6, B7 and B8, respectively, compared to the control beam B2. In the experimental results, the failure load of **group (B)** increased by (73, 78 and 86.6%) compared to the control beam B2. This group of beams was reinforced with 3 Ø 12 as longitudinal steel reinforcement (0.75% steel reinforcement).

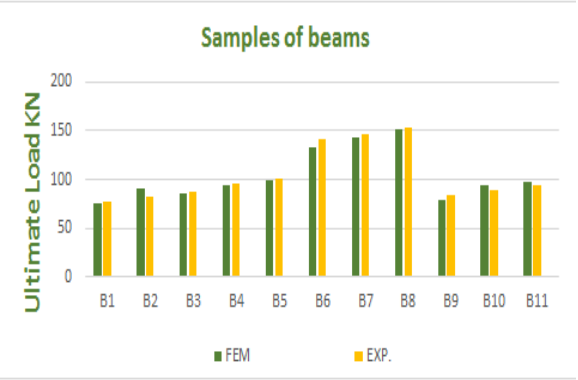

Fig 14. Comparison of the ultimate load between FEM & EXP

6.3 Crack patterns

Fig.'s (15 & 16 & 17) show the crack patterns from both the experimental testing and the numerical model. It was found that the numerical model efficiently predicts the beam behavior when compared with the experimental results. The ANSYS program records a crack pattern at each applied load step. Crack shape and size indicate that the flexure failure mode took place. The first crack began to appear at mid-span of the beam at the lower part, then was followed by cracks towards the supports. As shown in the figures, cracking was similar for both Exp. and FEA.

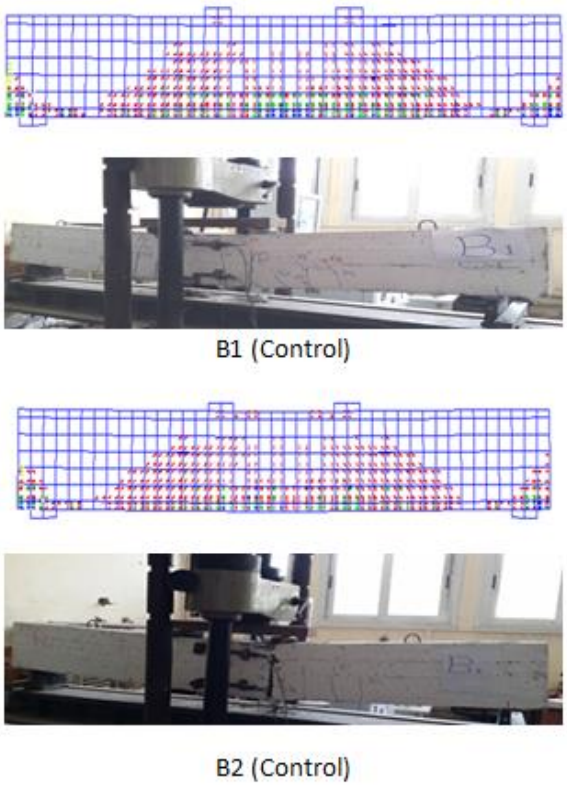

Fig 15. Crack pattern of the FEM and experimental tested beams.

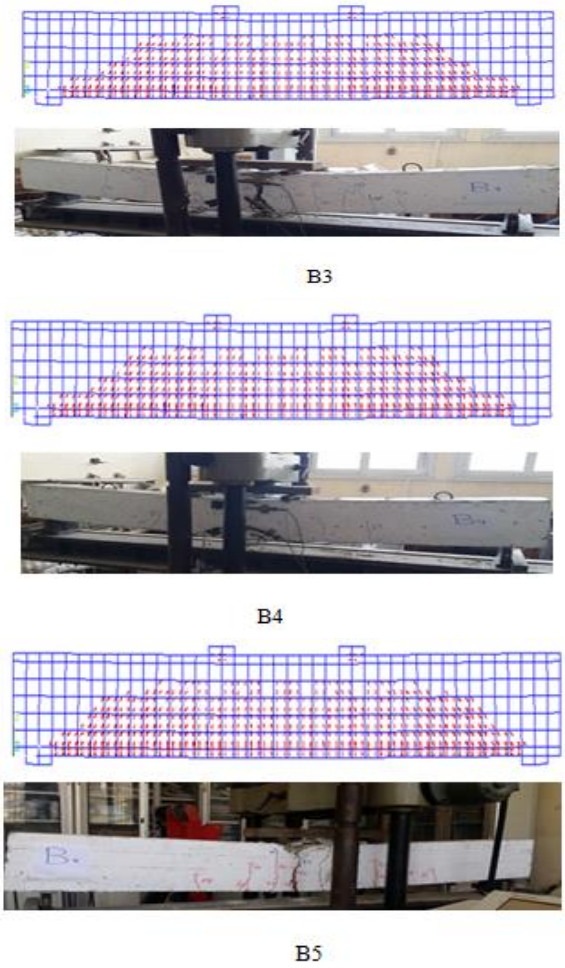

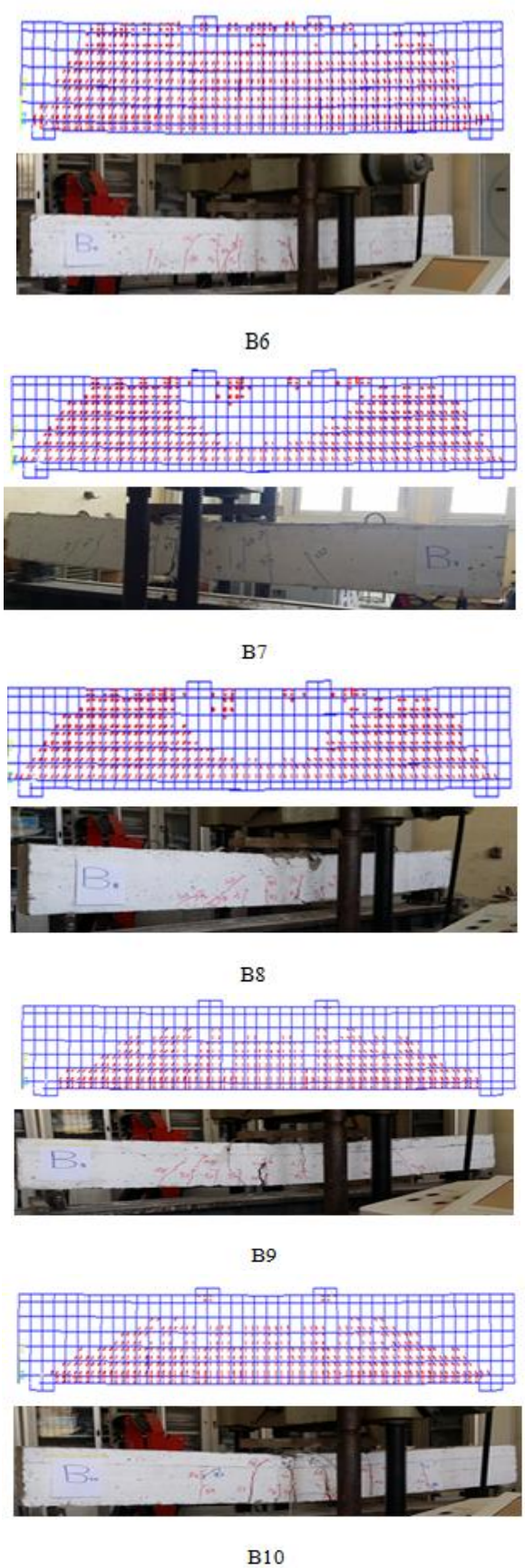

Fig 16. Crack pattern of the FEM and experimental tested beams.

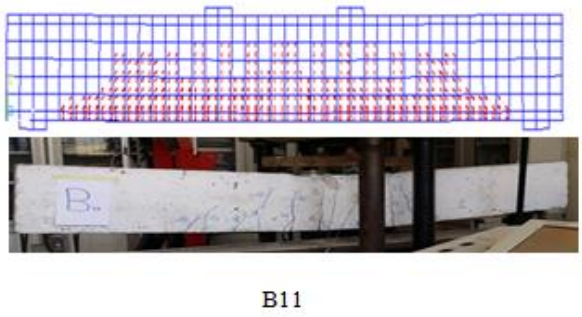

Fig 17. Crack pattern of the FEM and experimental tested beams.

7 Description of the parametric studies and analyzed beams

A parametric study was carried out using the finite element package ANSYS 15. A total of 85 similar beam specimens were investigated. The 85 beam specimens may be classified into 15 groups . All beams had dimensions of 150 mm width, 300 mm depth, and 2100 mm length. The beams were simply supported with a 1900 mm clear span. The load-deflection curve, energy absorption (toughness), failure modes and crack patterns were studied.

- **Groups (1, 2 and 3)** consisted of 15 beams reinforced with a volume of steel fiber (0.5%) and uniaxial geogrid volumetric ratio ranging between 3.0% to 9.0%, respectively, and with different concrete strengths = 25, 35 and 45 MPa. The bottom reinforcement ratio was equal to 0.25%. This study aimed to investigate the effect of using different values of Geogrids on the behavior of beams with different values of compressive strength.
- **Groups (4 and 5)** had different ratios of steel fiber vf % varying from 0.5% to 1.5%. Group 4 was reinforced with uniaxial geogrid volumetric ratio of 3.0% and bottom reinforcement ratio of 0.25%. Group 5 was reinforced with a uniaxial geogrid volumetric ratio of 9.0% and bottom reinforcement ratio equal to 1.5% having a concrete strength equal to 35 MPa. This study aimed to investigate the effect of varying the steel fiber ratio with min and max geogrid volumetric ratio and min. and max. bottom reinforcement ratios.
- **Groups (6 to 10)** These groups were reinforced by geogrid volumetric ratios ranging between (3% to 9%) and bottom reinforcement ratio from (0.25% to 1.5%) with a concrete strength =35 MPa and a volume of steel fiber (1.0%). This study aimed to investigate the effect of increasing the geogrid volumetric ratio with different bottom reinforcement ratios.
- **Groups (11 to 15)** These groups were reinforced with different steel fiber Vf ranging between (0.5% to 1.5%) with a bottom reinforcement ratio ranging between (0.25% to 1.5%) with a concrete strength

equal to 35 MPa and uniaxial geogrid volumetric ratio equal to 3.0%. This study aimed to investigate the effect of increasing the volumetric ratio of steel fibers with different values of bottom reinforcement ratios.

Tables (4 & 5&6) illustrate the details of the parametric study.

Table 4 Description of beam models

group	Beam specimen	Concrete compressive strength Fcu (MPa)	Steel fiber Vf (%)	Geogrid volumetric ratio µG (%)	Bottom Reinforcement Ratio
1	S1-25	25	0.50 %	3%	0.25%
	S2-25			4.5%	
	S3-25			6%	
	S4-25			7.5%	
	S5-25			9%	
2	S6-35	35	0.50 %	3%	0.25%
	S7-35			4.5%	
	S8-35			6%	
	S9-35			7.5%	
	S10-35			9%	
3	S11-45	45	0.50 %	3%	0.25%
	S12-45			4.5%	
	S13-45			6%	
	S14-45			7.5%	
	S15-45			9%	
4	S16	35	0.5%	3.0%	0.25%
	S17		0.75 %		
	S18		1.0%		
	S19		1.25 %		
	S20		1.5%		
5	S21	35	0.5%	9.0%	1.5%
	S22		0.75 %		
	S23		1.0%		
	S24		1.25 %		
	S25		1.5%		

Table 5 Description of beam models

group	Beam specimen	Concrete compressive strength Fcu (MPa)	Steel fiber Vf (%)	Geogrid volumetric ratio µG (%)	Bottom Reinforcement Ratio
6	S26	35	1%	3%	0.25%
	S27				0.50%
	S28				0.75%
	S29				1%
	S30				1.25%
	S31				1.5%
7	S32	35	1%	4.5%	0.25%
	S33				0.50%
	S34				0.75%
	S35				1%
	S36				1.25%
	S37				1.5%
8	S38	35	1%	6%	0.25%
	S39				0.50%
	S40				0.75%
	S41				1%
	S42				1.25%
	S43				1.5%
9	S44	35	1%	7.5%	0.25%
	S45				0.50%
	S46				0.75%
	S47				1%
	S48				1.25%
	S49				1.5%
10	S50	35	1%	9.0%	0.25%
	S51				0.50%
	S52				0.75%
	S53				1%
	S54				1.25%
	S55				1.5%

Table 6 Description of beam models

group	Beam specimen	Concrete compressive strength Fcu (MPa)	Steel fiber Vf (%)	Geogrid volumetric ratio µG (%)	Bottom Reinforcement Ratio
11	S56	35	0.5 %	3.0%	0.25%
	S57				0.50%
	S58				0.75%
	S59				1%
	S60				1.25%
	S61				1.5%
12	S62	35	1.0 %	3.0%	0.25%
	S63				0.50%
	S64				0.75%
	S65				1%
	S66				1.25%
	S67				1.5%
13	S68	35	1.5 %	3.0%	0.25%
	S69				0.50%
	S70				0.75%
	S71				1%
	S72				1.25%
	S73				1.5%
14	S74	35	2.0 %	3.0%	0.25%
	S75				0.50%
	S76				0.75%
	S77				1%
	S78				1.25%
	S79				1.5%
15	S80	35	2.5 %	3.0%	0.25%
	S81				0.50%
	S82				0.75%
	S83				1%
	S84				1.25%
	S85				1.5%

7.1 Effect of using different values of Geogrids with different compressive strengths:

This section studied three different concrete strengths; 25, 35 and 45 MPa, as shown in Table 4. The behavior of the beams is clarified by the load-deflection curves of the finite element analysis for the beams of groups (1, 2 and 3) as shown in Fig. 18.

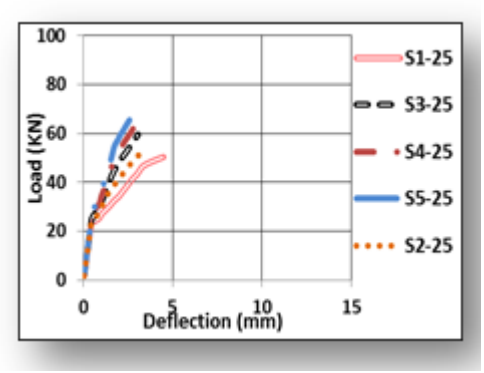

(a)Load-deflection curve of a group (1)

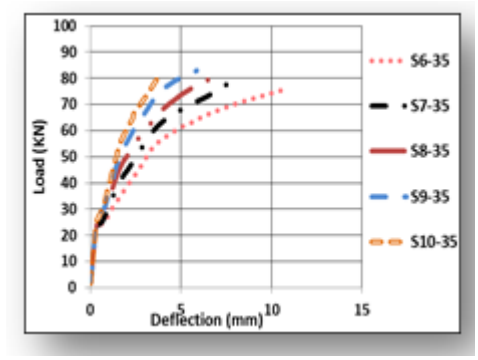

(b) Load-deflection curve of a group (2)

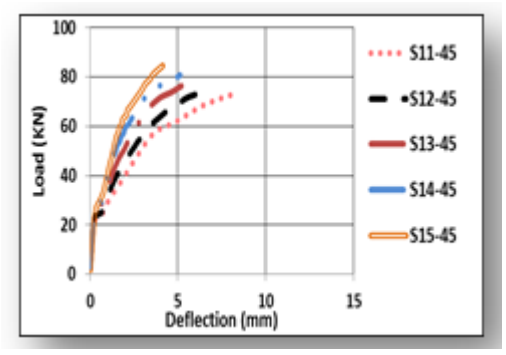

(c) Load-deflection curve of a group (3)

Fig 18. Analytical Load-deflection curves showing the effect of different Geogrid values on behavior of beams with different compressive strength groups 1, 2 and 3.

Table 7. Analytical Results For Beam Specimens for Groups (1 ,2 &3)

Group No	Specimen No.	Ultimate Load Pu (KN)	Percentage of increasing in (Pu%), as compared with the	Deflection (mm)	Percentage of decreasing in (&u), in comparison to the reference	Energy Absorption (Toughness) KN.mm
1	S1-25	50.4	——	4.48	——	230.664
	S2-25	52.2	3.6	3.19	28.8	165.146
	S3-25	59.4	17.9	3.07	31.5	170.438
	S4-25	64.8	28.6	3.00	33	171.409
	S5-25	72	43	3.2	28.6	219.068
2	S6-35	77.4	——	11.73	——	976.14
	S7-35	79	2.07	7.85	33	637.3
	S8-35	82	5.9	7.23	38.4	609.12
	S9-35	82.8	6.5	5.89	49.7	502.18
	S10-35	81	2.25	3.89	66.8	311.22
3	S11-45	73.8	——	8.5	——	657.07
	S12-45	75.6	2.4	6.98	17.9	544.82
	S13-45	79.2	7.3	5.95	30	484.09
	S14-45	81	9.75	5.14	39.5	422.5
	S15-45	84.6	14.6	4.13	51.4	257.39

7.1.1 Load Deflection behavior:

Deflection is measured at mid-span at the bottom side for all beams. The deflection was increased linearly by increasing the load until the failure load. The numerical calculation ended at the point of the ultimate load because the used stress-strain curve doesn't include concrete post behavior. The maximum deflection is determined at mid-span. Fig. (18) and table (7) show the load-deflection relations for groups 1, 2 and 3.

- In group 1, the maximum deflection equals 4.48 mm, 3.19 mm, and 3.07 mm, corresponding to the failure load at 50.4 KN, 52.2 KN, and 59.4 KN for beams s1-25, s2-25 and s3-25, respectively.
- In group 2, the maximum deflection equals 11.73 mm, 7.85 mm, and 7.23 mm, corresponding to the failure load at 77.4 KN, 79 KN, and 82 KN for beams s6-35, s7-35 and s8-35, respectively
- In group 3, the maximum deflection equals 8.5 mm, 6.98 mm, and 5.95 mm, corresponding to the failure load at 73.8 KN, 75.6 KN, and 79.2 KN for beams s11-45, s12-45 and s13-45, respectively.

Thus, increasing the geogrid volumetric ratio significantly increased the failure loads of the specimens. The effect of addition of Geogrids was more pronounced in group (1) with compressive strengths equal 25 MPa.

7.1.2 Energy Absorption (Toughness)

It was calculated as the area under the load-deflection curves up to the fracture of the beams.

- **For group (1):** The toughness of beam s2-25 was decreased by 28.4% compared to s1-25. For Beams s3-25, s4-25, and s5-25, the toughness was less than s1-25 by 26.1%, 25.7%, and 5.03% respectively.
- **For group (2):** The toughness of beams s7-35, s8-35, s9-35 and s10-35 was less than s6-35 by 34.7%, 37.6%, 48.6%, and 68% , respectively.
- **For group (3):** The toughness of beams s12-45, s13-45, s14-45, and s15-45 was less than s11-45 by 17%, 26.3%, 35.7%, and 60.8% respectively.

7.1.3 Deflections:

- Fig. 18a indicates that the deflections of group (1) were decreased by 28.8%, 31.5 %, 33% and 28.6% for beams (s2-25), (s3-25), (s4-25) and (s5-25), respectively; compared to the specimen (s1-25). Fig. 18b shows that the deflections of group (2) were decreased by 33%, 38.4%, 49.7% and 66.8% for beams

(s7-35), (s8-35), (s9-35) and (s10-35), respectively; compared to the specimen s6-35. Fig. 18c, indicates that the deflection of group (3) were decreased by 17.9%, 30%, 39.5% and 51.4% for beams (s12-45), (s13-45), (s14-45) and (s15-45), respectively; compared to the specimen s11-45.

- **For beams** (s1-25), (s2-25), (s3-25), (s4-25) and (s5-25), the maximum deflection recorded is 4.48 mm at a failure load of 50.4 KN for beam (s1-25) with geogrid volumetric ratio 3%. By increasing the geogrid volumetric ratio to 9%, the failure load increased to 72 KN in beam (s 5-25) and the deflection decreased to 3.2mm.
- **For beams** (s6-35), (s7-35), (s8-35), (s9-35) and (s10-35), the maximum deflection recorded is 11.73 mm at a failure load of 77.4 KN for beam (s6-35) with geogrid volumetric ratio 3%. By increasing the geogrid volumetric ratio to 9% in beam (s10-35) the failure load increased to 81 KN and the deflection decreased to 3.89mm
- **For beams** (s11-45), (s12-45), (s13-45), (s14-45) and (s15-45), the maximum deflection recorded is 8.5 mm at a failure load of 73.8 KN for beam (s11-45) with geogrid volumetric ratio 3%. By increasing the geogrid volumetric ratio to 9% in beam (s15-45), the failure load increased to 84.6 KN and the the deflection decreased to 4.13mm

Thus, increasing the geogrid volumetric ratio significantly decreased the deflections at failure loads. The effect of addition of Geogrids was more pronounced in in group (2) with compressive strengths equal 35 MPa.

7.1.4 Crack patterns:

Fig.'s (19 and 20) show the crack patterns for specimens S1-25 and S11-45 with compressive strength 25 MPa and 45 MPa, respectively. The crack shape and size indicated that flexure failure mode took place. The first crack began to appear at the mid-span of the beam at the lower part, followed by cracking towards the supports. The cracks propagated by increasing the applied load as inclined lines in the maximum moment region. By increasing the load, more flexural cracks were formed until the failure of the beam. The ultimate flexural loads of these beams was 50.4 KN and 73.8 KN, respectively.

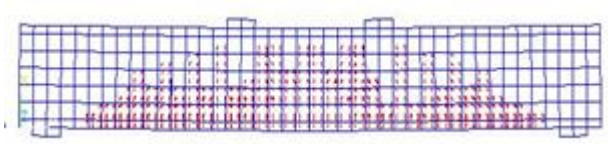

Fig 19. Crack pattern for s1-25

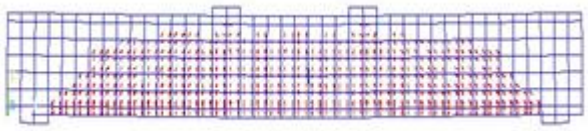

Fig 20. Crack pattern for s11-45

7.2 Effect of Increasing Percentages Steel Fibers on beams with min and max geogrid volumetric ratio and bottom reinforcement ratios:

The behaviour of the beams is verified by the load deflection curves of the finite element analysis for groups (4 and 5) as shown in Fig. 21.

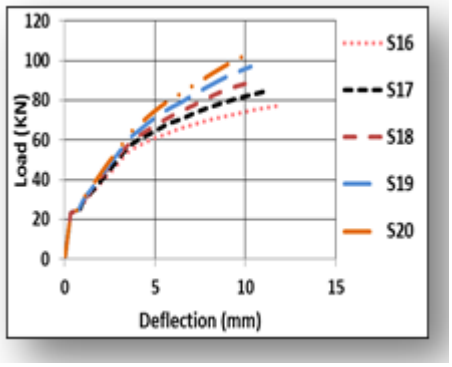

Load-deflection curve of a group (4)

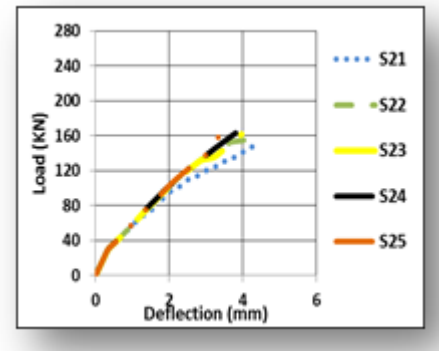

Load-deflection curve of a group(5)

Fig 21. Analytical Load-deflection curves showing the effect of min and max geogrid volumetric ratios with min. and max. Bottom Reinforcement Ratio groups 4 and 5

Table 8. Analytical Results For Beam Specimens of Groups (4 and 5)

GROUP NO `	SPECIMEN NO.	ULTIMATE LOAD Pu (KN)	Percentage of increasing in (Pu%), as compared with the reference	DEFLECTION (mm)	Percentage of decreasing in (&u), in comparison to the reference	Energy Absorption (Toughness) KN.mm
	S16	77.4	——	11.73	——	976.14
	S17	84.6	9.3	11.20	4.5	987
	S18	90	14	10.55	10	974.6
	S19	97	25.3	10.28	12.4	999.2
4	S20	102.6	32.6	9.99	14.8	1012.5
	S21	149.4	——	4.35	——	605.26
	S22	158.4	6.02	4.18	4.07	606.9
	S23	162	8.43	3.96	9.33	580.8
	S24	165.6	10.84	3.89	11	580.5
5	S25	172.8	15.66	3.74	14.59	572.4

7.2.1 **Load Deflection behavior**

The load deflection curves of the finite element analysis for groups (4 and 5) are shown in Fig. (21) and table (8).

- In group 4, the maximum deflection equals 11.73 mm, 11.20 mm and 10.55 mm, corresponding to the failure load at 77.4 KN, 84.6 KN and 90 KN for beams S16, S17 and S18, respectively. Fig. 23a indicates that the deflection of group (4) decreased by 4.5%, 10 %, 12.4 and 14.8% for beams s17, s18, s19 and s20 respectively; compared to the specimen s16.
- In group 5, the maximum deflection equals 4.35 mm, 4.18 mm, and 3.96 mm, corresponding to the failure load at 149.4 KN, 158.4 KN, and 162 KN for beams S21, S22 and S23, respectively. Fig. 23b indicates that the deflection of group (5) decreased by 4.07%, 9.33%, 11% and 14.59% for beams s22, s23, s24 and s25, respectively, compared to the specimen s21.

7.2.2 **Energy Absorption (Toughness)**

- **For group (4):** The toughness for beams s17, S18, s19 and s20 were higher than s16 by 1.11%, 2. 3% and 3.7% respectively.
- **For group (5):** The toughness for beams s22, s23, s24 and s25 were lower than s21 by 0%, 4.09 %, 4.1% and 5.48% respectively.

7.2.3 **Failure Loads:**

Fig. 21 shows the effect of increasing the steel fibers from (0.5% to 1.5%) on the failure loads of the beams with minimum and maximum geogrid volumetric ratio and Bottom Reinforcement Ratio, with constant fcu=35MPa.

- Fig. 21a indicates that the failure load of group (4) were increased by 9.3%, 14%, 25.3%, and 32.6% for beams s17, s18, s19 and s20 respectively; compared to the specimen s16.
- Fig. 21b shows that the failure load of a group (5) were increased by 6.02%, 8.43%, 10.84% and 15.66% for beams s22, s23, s24 and s25, respectively, compared to the specimen s21.

Thus, the addition of 1% steel fibers with low values of both Geogrid and Bottom Steel Ratios resulted in an increase of 32.6 % in ultimate load and a decrease of 14.8% in deflection. High values of both Geogrid and Bottom Steel Ratios in the presence of 1% steel fibers resulted in an increase of 15.4 % in ultimate load and decrease of 14% in deflection.

7.2.4 Crack patterns:

Fig.'s (22 and 23) for specimen s16 & S20 with 0.5% & 1.5% steel fiber, respectively show the crack patterns for both beams. The crack shape and size indicate that flexural failure mode took place. The first crack began to appear at the mid-span of the beam at the lower part, followed by cracking towards the supports. The cracks propagated by increasing the applied load as inclined lines in the maximum moment region. By increasing the load, more flexural cracks were formed until the failure of the beams. The ultimate flexural loads for these beams were 77.4 KN and 102.6 KN respectively.

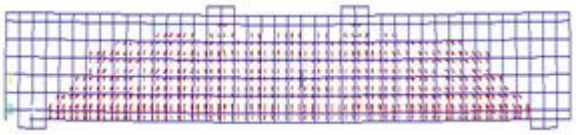

Fig 22. Crack pattern for s16

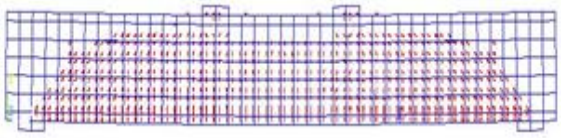

Fig 23. Crack pattern for s20

7.3 Effect of Increasing Geogrid volumetric ratio with different Bottom Reinforcement Ratios:

The effect of increasing Geogrid volumetric ratio from (3% to 9%) with different Bottom Reinforcement Ratio ranging between (0.25% to 1.5%) is here-in discussed. The values of the concrete strength =35 MPa and volume of steel fiber Vf= 1.0%. Fig. 24 shows the load deflection curves of the finite element analysis for groups (from 6 to 10).

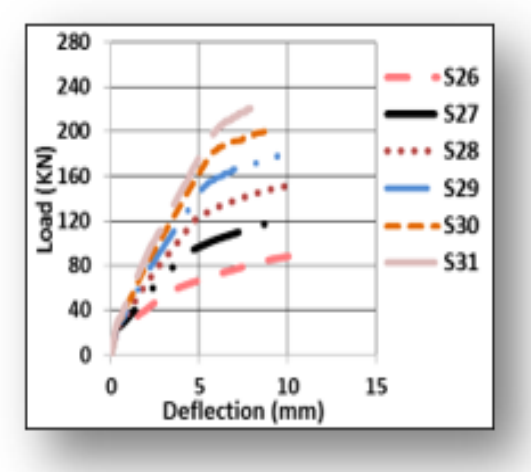

Load-deflection curve of a group (6)

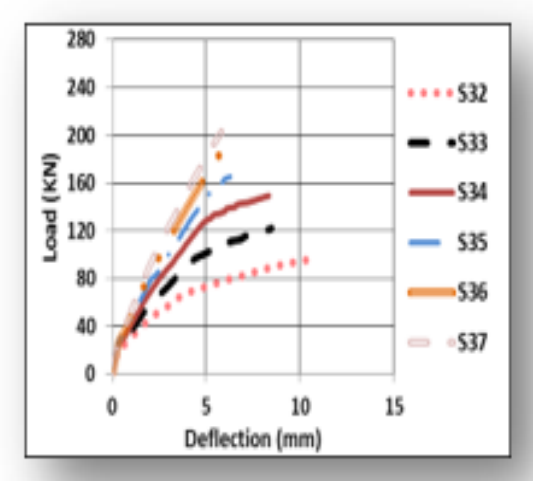

Load-deflection curve of a group (7)

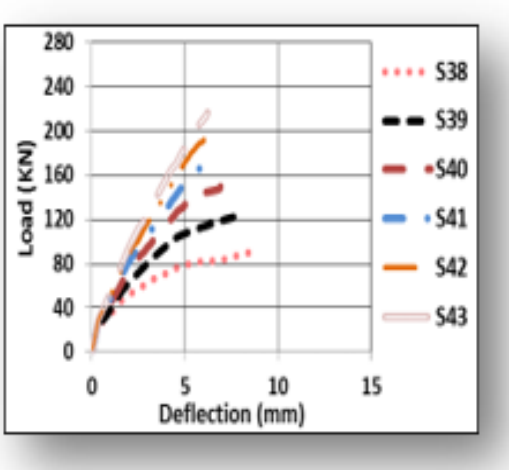

Load-deflection curve of a group (8)

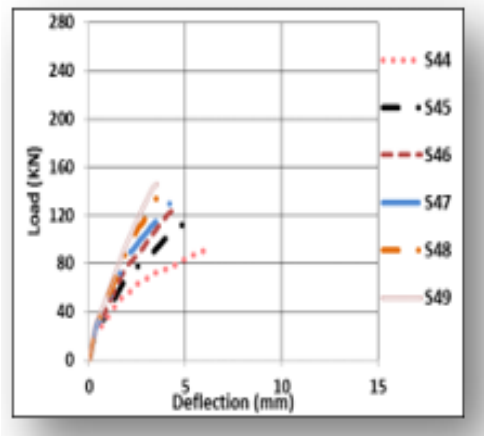

Load-deflection curve of a group (9)

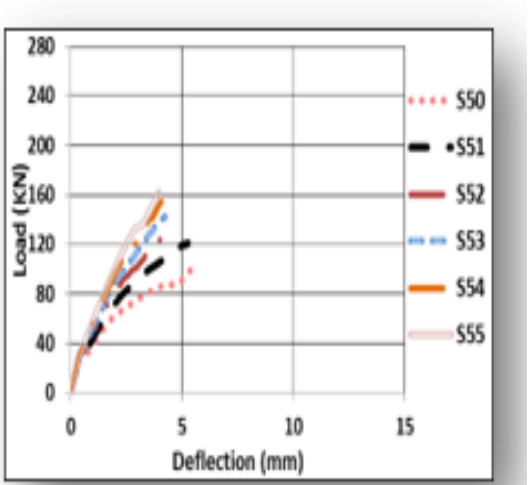

(e)Load-deflection curve of a group (8)

Fig 24. Analytical Load-deflection curves showing the effect of increasing Geogrid volumetric ratio with different bottom reinforcement Ratios and for groups 6 to10.

Table 9. Analytical Results For Beam Specimen and Discussion for Groups (6 to 10)

GROUP NO	SPECIMEN NO.	LOAD Pu (KN)	Percentage of increasing in (Pu%), as compared with the reference	DEFLECTION (mm)	Percentage of decreasing in (&u), in comparison to the reference	Energy Absorption (Toughness) KN.mm
6	S26	90	——	10.55	——	974.63
	S27	122.4	36	10.2	3.3	1226.09
	S28	151.2	68	10.03	4.9	1443.74
	S29	178.2	98	9.42	10.7	1565.82
	S30	201.6	124	8.73	17.25	1609.97
	S31	223.2	148	8.2	22.27	1662.108
7	S32	97.2	——	10.87	——	1098.83
	S33	122.4	20.6	8.5	21.8	1015.4
	S34	149.4	53.7	8.33	23.4	1170
	S35	165.6	70.4	6.29	42.1	953.8
	S36	189	94.4	5.96	45.2	1010.77
	S37	203.4	109	5.79	46.7	1035.5
8	S38	90	——	8.50	——	805.99
	S39	122.4	36	7.63	10.2	909.09
	S40	149.4	66	6.92	18.59	970.1
	S41	172.8	92	6.45	24.1	1019.03
	S42	194.4	116	6.23	26.7	1093.96
	S43	216	140	6.20	27.06	1200.82
9	S44	91.8	——	6.15	——	572.96
	S45	115.2	25.5	5.09	17.2	558.33
	S46	126	37.25	4.4	28.46	509.09
	S47	129.6	41.2	4.2	31.7	502.5
	S48	140.4	52.9	3.67	40.33	464.57
	S49	145.8	58.8	3.5	43.09	461.227
10	S50	102.6	——	5.54	——	558.3
	S51	120.6	17.5	5.29	4.5	608.4
	S52	135	31.6	4.45	19.7	563.7
	S53	142.2	38.6	4.23	23.6	561.2
	S54	154.8	50.9	4.07	26.5	568.3
	S55	162	57.89	3.96	28.52	580.8

7.3.1 Load Deflection behavior

The maximum deflection is determined at mid-span of the beams. The deflection increased linearly by increasing the load until the failure load. Fig.'s (24) and table (9) show the load-deflection relations for groups from 6 to 10.

- In group 6, the maximum deflection equals 10.55 mm, 10.2 mm, and 10.03 mm, 9.42 mm, 8.73 mm, 8.2mm, corresponding to the failure load at 90 KN, 122.4 KN, 151.2 KN, 178.2 KN, 201.6 KN, 223.2 KN, for beams s26, s27and s28, S29, S30, S31 respectively.
- In group 7, the maximum deflection equal 10.87 mm, 8.5 mm, and 8.33 mm, 6.29 mm, 5.96 mm, 5.79 mm, corresponding to the failure load at 97.2 KN, 122.4 KN, and 149.4,165.6 KN , 189 KN, 203.4 KN for beams s32, s33and s34, S35, S36, S37 respectively.
- In group 8, the maximum deflection equals 8.5 mm, 7.63 mm, and 6.92 mm, 6.45 mm, 6.23 mm, 6.20 mm, corresponding to the failure load at 90 KN, 122.4 KN, and 149.4 KN , 172.8 KN , 194.4 KN, 216 KN for beams s38, s39and s40, S41 , S42 ,S43, respectively.

- In group 9, the maximum deflection equals 6.15 mm, 5.09 mm, and 4.4 mm, 4.2 mm, 3.67 mm, 3.5 mm, corresponding to the failure load at 91.8 KN, 115.2 KN, and 126 KN, 129.6KN, 140.4 KN, 145.8 KN, for beams s44, s45 and s46, S47, S48, S49, respectively.
- In group 10, the maximum deflection equals 5.54 mm, 5.29 mm, and 4.45 mm, 4.23 mm, 4.07 mm, 3.96 mm, corresponding to the failure load at 102.6 KN, 120.6 KN, and 135 KN for beams s50, s51 and s52, S53, S54, S55, respectively.

7.3.2 Energy Absorption (Toughness)

- **For group (6):** beams s27, s28, s29, s30 and s31 was bigger than s26, respectively, by 25.8%, 48%, 60.7%, 65% and 70.5%.
- **For group (7):** beams s33, s35, s36 and s37 was smaller than s32, respectively, by 7.6%, 13.5%, 8% and 5.8%.
- **For group (8):** beams s39, s40, s41, s42 and s43 was bigger than s38, respectively, by 12.8%, 20.4%, 26.4%, 35.7% and 48.99%.
- **For group (9):** beams s45, s46, s47, s48 and s49 was smaller than s44, respectively, by 2.6%, 11.14%, 12.3%, 18.9% and 19.5%.
- **For group (10):** beams s51, s52, s53, s54 and s55 was smaller than s50, respectively, by 8.9%, 0.97%, 0.52%, 1.79% and 4%.

7.3.3 Failure Loads:

The effect of increasing the geogrid volumetric ratio from (3% to 9%) and Bottom Reinforcement Ratio from (0.25% to 1.5%) with constant concrete strength =35 MPa and a volume of steel fiber Vf (1.0%); on the failure loads of the beams is here-in presented:

- Fig. 24a indicates that the deflections of group (6) with geogrid volumetric ratio = 3% were decreased by 3.3%, 4.9 %, 10.7, 17.25% and 22.27% for beams s27, s28, s29, s30 and s31 respectively; compared to specimen s26.
- Fig. 24b shows that the deflection of group (7) with geogrid volumetric ratio = 4.5% were decreased by 21.8%, 23.4%, 42.1 %, 45.2and 46.7% for beams s33, s34, s35, s36 and s37 respectively; compared to specimen s32.
- Fig. 24c indicates that the deflection of group (8) with geogrid volumetric ratio = 6% were decreased by 10.2%, 18.59%, 24.1 %, 26.7 and 27.06 % for beams s39, s40, s41, s42 and s43 respectively; compared to specimen s38.
- Fig. 24d indicates that the deflection of group (9) with geogrid volumetric ratio = 7.5% were decreased by 17.2%, 28.46%, 31.7 %, 40.33 and 43.09 % for beams s45, s46, s47, s48 and s49 respectively; compared to specimen s44.
- Fig. 24e shows that the deflection of group (10) with geogrid volumetric ratio = 9% were decreased by 4.5%, 19.7%, 23.6 %, 26.5 and 28.52 % for beams s51, s52, s53, s54 and s50 respectively; compared to the specimen s44.
- **For group (6)** beams with geogrid volumetric ratio 3%: the maximum deflection recorded is 10.55 mm at a failure load of 90 KN for beam (s26). By increasing the bottom reinforcement ratio to 1.5% in beam (s31), the failure load increased to 223.2 KN and, the deflection decreased to 8.2mm.
- **For group (7)** with geogrid volumetric ratio 4.5%**:** the maximum deflection recorded is 10.87 mm at a failure load of 97.2 KN for beam (s32). By increasing the bottom reinforcement ratio to 1.5% in beam (s37), the failure load increased to 203.4 KN, the deflection decreased to 5.79mm.
- **For group (8)** beams with geogrid volumetric ratio 6%, the maximum deflection recorded is 8.5 mm at a failure load of 90 KN for beam (s38). By increasing the bottom reinforcement ratio to 1.5% in beam (s43), the failure load increased to to 216 KN and the deflection decreased to 6.20 mm.
- **For group (9):** beams with geogrid volumetric ratio 7.5%, the maximum deflection recorded is 6.15 mm at a failure load of 91.8 KN for beam (s44). By increasing the bottom reinforcement ratio to 1.5% in beam (s49), the failure load increased to to 145.8 KN and the deflection decreased to 3.5mm.
- **For group (10)** beams with geogrid volumetric ratio 9%, the maximum deflection recorded is 5.54 mm at a failure load of 102.6 KN for beam (s50). By increasing the bottom reinforcement ratio to 1.5%, the failure l oad increased to 162 KN in beam (s55) and the deflection decreased to 3.96 mm.

7.3.4 Crack patterns:

Fig.'s (25 and 26) show the crack patterns for specimens s26 and s50 with minimum and maximum geo-grid volumetric ratios of 3% and 9 % respectively. The crack shape and size indicated that the flexural failure mode took place. The first crack began to appear at the mid-span of the beam at the lower part, followed by cracking towards the supports. The cracks propagated by increasing the applied load as inclined lines in the maximum moment region. By increasing the load, more flexural cracks were formed until the failure of the beam. The ultimate flexural load of these beams were 90 KN and 102.6 KN respectively.

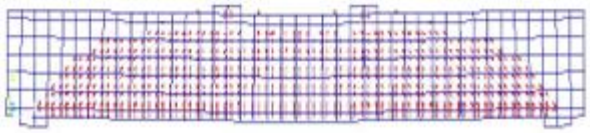

Fig 25. Crack pattern for s26

Fig 26. Crack pattern for s50

7.4 Effect of Increasing the steel fiber Vf with Different Bottom Reinforcement Ratios:

The effect of increasing the steel fiber Vf from (0.5% to 1.5%) with varying Bottom Reinforcement Ratio from (0.25% to 1.5%) is here-in presented .The concrete strength and uniaxial geogrid volumetric ratio were kept constant.
Fig.'s (27 and 28) show the load deflection curves resulting from the finite element analysis for groups (11 to 15).

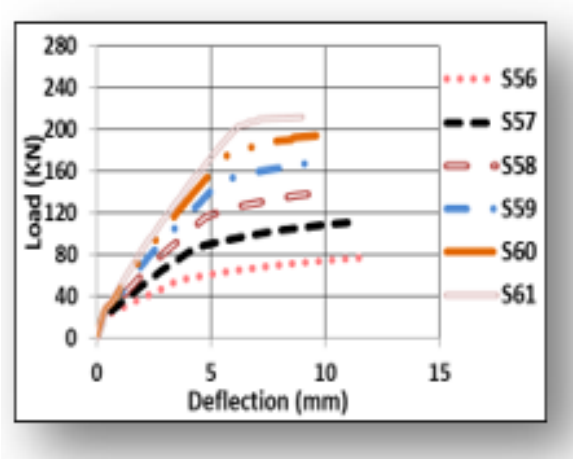

(a) Load-deflection curve of a group (11)

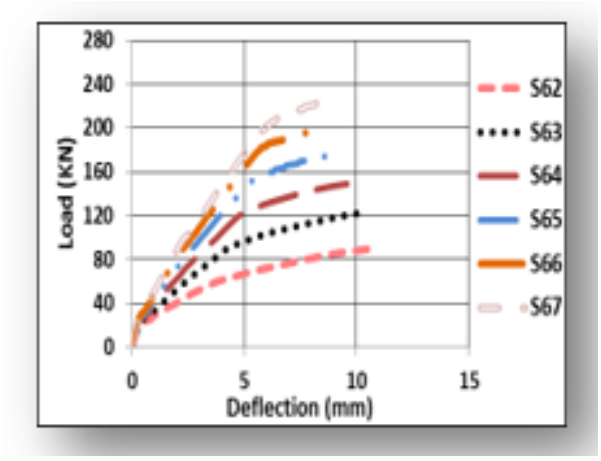

(b) Load-deflection curve of a group (12)

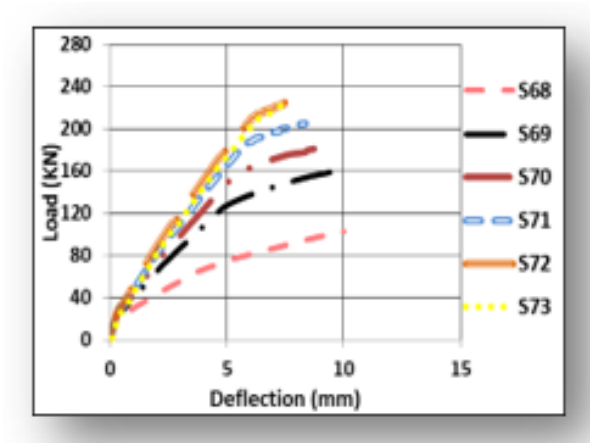

(c) Load-deflection curve of a group (13)

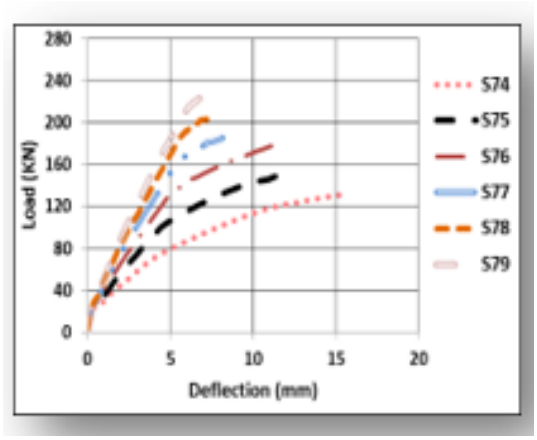

(d) Load-deflection curve of a group (14)

Fig 27. Analytical Load-deflection curves showing the effect increasing the steel fiber Vf with different bottom reinforcement ratios groups 11 and 15.

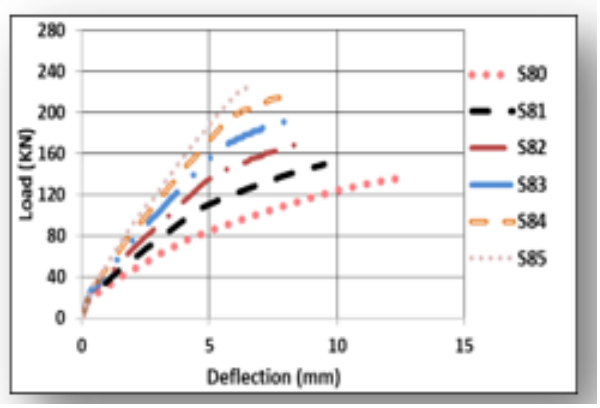

(e) Load-deflection curve of a group (15)

Fig 28. Analytical Load-deflection curves showing the effect increasing the steel fiber Vf with different bottom reinforcement ratios groups 11 and 15.

Table 10. Analytical Results For Beam Specimen for Groups (11 to 15)

GROUP NO	SPECIMEN NO.	LOAD Pu (KN)	Percentage of increasing in (Pu%), as compared with the reference	DEFLECTION (mm)	Percentage of decreasing in (&u), in comparison to the reference	Energy Absorption (Toughness) KN.mm
11	S56	77.4	——	11.73	——	976.14
	S57	111.6	44.19	10.99	6.3	1229.97
	S58	140.4	81.4	10.18	13.2	1372.62
	S59	171	120.9	9.7	17.3	1551.19
	S60	194.4	151.16	9.6	18.16	1723.14
	S61	212.4	174.4	8.97	23.5	1741.5
12	S62	90	——	10.55	——	974.63
	S63	122.4	36	10.2	3.3	1226.09
	S64	151.2	68	10.03	4.9	1443.74
	S65	178.2	98	9.42	10.7	1565.82
	S66	201.6	124	8.73	17.25	1609.97
	S67	223.2	148	8.2	22.27	1662.108
13	S68	102.6	——	9.99	——	1012.5
	S69	160.2	56.14	9.7	2.9	1466.88
	S70	187.2	82.5	9.4	5.9	1629.4
	S71	205.2	100	8.34	16.5	1561.37
	S72	226.8	121	7.87	21.22	1611.67
	S73	228.6	122.8	7.53	24.6	1546.48
14	S74	131.4	——	15.32	——	2035.86
	S75	154.8	17.8	12.4	19.06	1868.02
	S76	180	36.99	11.59	24.35	1980.62
	S77	185.4	41.09	8.17	46.67	1404.42
	S78	207	57.53	7.72	49.61	1445.33
	S79	225	71.23	7.07	53.85	1424.47
15	S80	136.8	——	12.65	——	1668.75
	S81	149.4	9.21	9.5	24.9	1336.52
	S82	172.8	26.3	8.97	29.09	1433.63
	S83	194.4	42.1	8.39	33.68	1490.63
	S84	214.2	56.58	7.77	38.58	1505.33
	S85	225	64.47	6.49	48.69	1298.58

7.4.1 Load Deflection behavior

Fig.'s (27 & 28) shows that the deflection was increased linearly by increasing the load until the failure load.

- In group 11, the maximum deflection equals 11.73 mm, 10.99 mm, and 10.18 mm, 9.7 mm, 9.6 mm, 8.97 mm, corresponding to the failure load at 77.4 KN, 111.6 KN, and 140.4 KN, 171 KN, 194.4 KN, 212.4 KN, for beams s56, s57 and s58, s59, s60, s61, respectively.
- In group 12, the maximum deflection equals 10.55 mm, 10.2 mm, and 10.03 mm, 9.42 mm, 8.73 mm, 8.2mm, corresponding to the failure load at 90 KN, 122.4 KN, and 151.2 KN,178.2 KN, 201.6 KN, 223.2 KN for beams s62, s63 and s64, s65, s66, s67 respectively.

- In group 13, the maximum deflection equals 9.99 mm, 9.70 mm, and 9.4 mm, 8.34 mm, 7.87 mm, 7.53 mm, corresponding to the failure load at 102.6 KN, 160.2 KN, and 187.2 KN, 205.2 KN, 226.8 KN, 228.6 for beams s68, s69 and s70, s71, s72, s73, respectively.
- In group 14, the maximum deflection equals 15.32mm, 12.4 mm, and 11.59 mm, 8.17 mm, 7.72 mm,7.07 mm, corresponding to the failure load at 131.4 KN, 154.8 KN, and 180 KN, 185.4 KN, 207 KN, 225 KN for beams s74, s75 and s76, s77, s78, s79 respectively.
- In group 15, the maximum deflection equals 12.65 mm, 9.5 mm, and 8.97 mm, 8.39 mm, 7.77 mm, 6.49 mm, corresponding to the failure load at 136.8 KN, 149.4 KN, and 172.8 KN, 194.4 KN, 214.2 KN, 225 KN for beams s80, s81 and s82, s83, s84, s85, respectively.

7.4.2 Energy Absorption (Toughness)

- **For group (11):** The toughness for beams s57, s58, s59, s60 and s61 was higher than s56 by 26%, 40.6%, 58.9%, 76.5% and 78.4%, respectively.
- **For group (12):** The toughness beams s63, s64, s65, s66 and s67 was higher than s62, by 25.8%, 48%, 60.7%, 65% and 70.5% respectively.
- **For group (13):** The toughness beams s69, s70, s71, s72 and s73 was higher than s68, by 44.9%, 60.9%, 54.2%, 59.2% and 52.7% respectively.
- **For group (14):** The toughness beams s75, s76, s77, s78 and s79 was less than s74, by 8.2%, 2.7%, 31%, 29% and 77.3% respectively.
- **For group (15):** The toughness beams s81, s82, s83, s84 and s85 was less than s80, by 19.9%, 14.08%, 10.7%, 9.8% and 22.2% respectively..

7.4.3 Failure Loads:

- Fig. 27a shows that the deflection of group (11) were decreased by 6.3%, 13.2%, 17.3%, 18.16% and 23.5% for beams s57, s58, s59, s60 and S61, respectively, compared to the specimen s56.
- Fig. 27b indicates that the deflection of group (12) were decreased by 3.3%, 4.9%, 10.7%, 17.25% and 22.27% for beams s63, s64, s65, s66 and 67, respectively, compared to the specimen s62.
- Fig. 27c, indicates that the deflection of the group (13) were decreased by 2.9%, 5.9%, 16.5%, 21.22% and 24.6% for beams s69, s70, s71, s72 and 73, respectively, compared to the specimen s68.
- Fig. 27d, shows that the deflection of the group (14) were decreased by 19.06%, 24.35%, 46.67%, 49.61% and 53.85% for beams s75, s76, s77, s78 and 79, respectively, compared to the specimen s74.
- Fig. 28e, indicates that the deflection of the group (15) were decreased by 24.9%, 29.09%, 33.68%, 38.58% and 48.69% for beams s81, s82, s83, s84 and 85, respectively, compared to the specimen s80.

- **For group (11)** for beams with Vf (0.5%), the maximum deflection is 11.73 mm at a failure load of 77.4 KN for beam (s56). By increasing the bottom reinforcement ratio to 1.5%, the failure load increased to 212.4 KN in beam (s61) and the deflection decreased to 8.97 mm.
- **For group (12)** for beams with Vf (1%), the maximum deflection is 10.55 mm at a failure load of 90 KN for beam (s62). By increasing the bottom reinforcement ratio to 1.5%, the failure load increased to 223.2 KN in beam (s67) and the the deflection decreased to 8.2 mm.
- **For group (13)** for beams with Vf (1.5%), the maximum deflection recorded is 9.99 mm at a failure load of 102.6 KN for beam (s68). By increasing the bottom reinforcement ratio to 1.5%, the failure load increased to 228.6 KN in beam (s73) and the deflection decreased to 7.53 mm.
- **For group (14)** for beams with Vf (2%), the maximum deflection is 15.32 mm at a failure load of 131.4 KN for beam (s74). By increasing the bottom reinforcement ratio to 1.5%, the failure load increased to 225 KN in beam (s79) and the deflection decreased to 7.07 mm.
- **For group (15)** for beams with Vf (2.5%), the maximum deflection is 12.65 mm at a failure load of 136.8 KN for beam (s80). By increasing the bottom reinforcement ratio to 1.5%, the failure load increased to 225 KN in beam (s85) and the deflection decreased to 6.49 mm.

7.4.4 Crack patterns:

Fig.'s (29 and 30) show the crack patterns for specimens s62 and s67, with minimum and maximum reinforcement ratios of 0.25% and 1.5% respectively. The crack shape and size indicated that the flexural failure mode took place. It is clear that the observed cracks were in the flexural zone at the mid-span, and the cracks propagated by increasing the applied load as inclined lines in the maximum moment region. By increasing the load, more flexural cracks were formed until the failure of the beam. The ultimate flexural loads of these beams were 90 KN and 223.2 KN respectively.

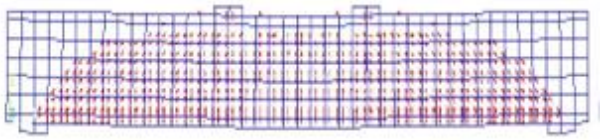

Fig 29. Crack pattern for s62

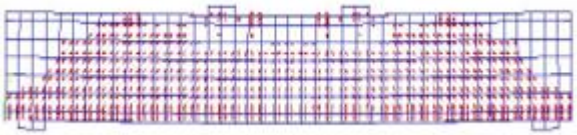

Fig 30. Crack pattern for s67

8 Conclusions:

Based on the theoretical and parametric studies, the following conclusions could be made:

1 The addition of uniaxial geogrids as a reinforcing technique proved to be an effective tool to improve the flexural behavior of beams and the cracking patterns.

2 Comparing the load-deflection curves from the analytical modeling and experimental results, it can be concluded that the numerical model efficiently predicts the ultimate strength and corresponding displacement compared with the experimental results. Since the differences between results are within an acceptable range; the FEA software ANSYS can be used effectively to analyze beams in which Geo-grid has been added as additional reinforcement.

3 The numerical model underestimated the ultimate strength of B1 by 1.8% compared with the experimental testing, while it overestimated the ultimate strength of B2 by 8.9% compared with experimental results.

4 For Group (A) beams (B3, B4, and B5), the analytical model underestimated the ultimate strengths by 1.8%, 1.5%, and 2 %, respectively, compared with the experimental tests. For Group (B) beams (B6, B7, and B8), the analytical model underestimated the ultimate strength by 6.2%, 1.4%, and 1.2 %, respectively, compared with the experimental testing. For Group (C) beams (B9, B10, and B11), the numerical model underestimated the ultimate strength of B9 by 5.7% and overestimated it in B10 and B11 by 5% and 3.3% compared with the experimental results.

5 The addition of geogrid layers in the specimens decreased the deflections of groups A, B, and C in the analytical model just as it was decreased in the experimental results compared to the control beam B2. By increasing the number of geogrid layers in group A, the deflection of B4 and B5 was decreased compared to B3. Also, in group C the deflection of B10 and B11 decreased compared to B9.

6 The ratio between the FEM compared to the EXP results of the first cracking load varies from 0.34 to 0.78. The ratio between the FEM compared to the experimental results of the ultimate load varies from 0.94 to 1.09. The ratio between the FEM to the experimental results of the deflection (at the same load level) varies from 0.70 to 1.09.

7 Increasing the geogrid volumetric ratio, in the presence of steel fibers, in reinforced concrete beams significantly decreases the deflection and increases the failure load of the beams.

8 For low percentages of bottom steel reinforcement, increasing the volumetric ratio of Geo-grid from 3% to 9% had a significant effect on deflection since it decreased by 47.5%. Also, failure load increased by 14%.

9 For high percentages of bottom steel reinforcement, increasing the volumetric ratio of Geo-grid from 3% to 9% had a significant effect on decreasing deflection since it decreased by 51.7%.

10 Increasing the steel fiber (Vf) ratio from 0.5% to 2.5% with minimum geogrid volumetric ratio of 3.0% had a considerable effect on decreasing the maximum deflections; since the deflection decreased by 27.6 %. On the contrary, this increase had a small effect on increasing the failure loads of the beams; since increasing steel fiber from (0.5% to 2.5%) increased the failure load from 212.4 KN to 225 KN by about 6%.

References

[1]. Saranyadevi M, Suresh M and Sivaraja M., (2016), "Strengthening of Concrete Beam by Reinforcing with Geosynthetic Materials" International Journal of Advanced Research in Education & Technology Vol.3, pp 2394-6814.

[2]. Reddy, M. P., and Kumar, R. K., (2018), "Study of geo-grid confined reinforced concrete beams", International Journal of Science, Engineering and Technology Research (IJSETR), Vol7, Issue 4, April, pp.278- 286.

[3]. Ramakrishnan S, Arun M, Loganayagan S, Mugeshkanna M.,(2018).Strength and Behavior of Geogrid Reinforced Concrete Beams International Journal of Civil Engineering 9(6) 1295- 1303

[4]. Martin Ziegler, (2017), "Application of geogrid reinforced constructions: history, recent and future developments" Procedia Engineering, vol. 172, pp. 42-51.

[5]. Chidambaram, R.S. and Agarwal, P., (2019), "Shear resistance behavior of geogrid-confined RC elements under static and cyclic loading", CSIR-Central Building Research Institute. CURRENT SCIENCE, 117(2), pp. 247-667.

[6]. Özkal FM., (2021), "Experimental investigation on the applicability of geogrid: A comparison between conventional and hybrid-

reinforced irregular reinforced concrete members", Advances in Structural Engineering, 24(8), pp.1497-1509.

[7]. Mona K.N Ghali et al., (2022), "Flexural Behavior of Reinforced Concrete Beams with Geogrid- Experimental Study", Engineering Research Journal(ERJ), 51(3), pp. 105-119.

[8]. ANSYS, (2015), Release 14.0 Documentation. ANSYS Inc., http://www.ansys.com.

[9]. Egyptian Code for Design of Reinforced Concrete Structures, No. 203/2020.

[10]. Rakendu, K., and Manoharan, A., (2017), "Flexural behavior of concrete beams reinforced with biaxial geogrid", International Journal of Engineering Research and General Science, Vol. 5, Issue 4, July-August, pp.72-83.

[11]. Ayman H. H. Khalil, Ashraf M. A. Heniegal, and Mohammed Mahmoud Attia, (2018), "Nonlinear Finite Element Analysis of Steel Fibers Reinforced Post-Tensioned Lightweight Concrete Beams". 11(6), pp. 80-92, ISSN 1554-0200 (print); ISSN 2375-723X (online).

[12]. Mr. Aniket Murekar, Mr. Durvesh Devikar, Mr. Jatin Singandhupe, Mohd. Faizan Farooqui and Mr. Sujesh Ghodmare., (2017), "Comparative Study and Analysis of PCC Beam and Reinforced Concrete Beam using Geogrid", International Journal of Science Technology & Engineering, Vol.3, pp. 2349-784X.